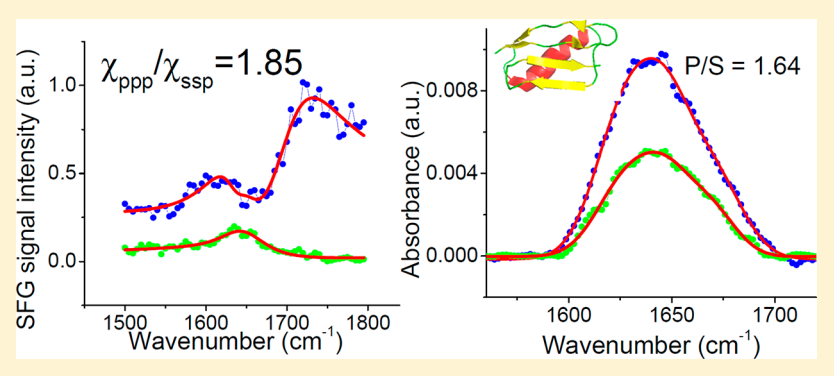


Control of Protein Conformation and Orientation on Graphene

Shuai Wei,[†] Xingquan Zou,^{†©} Jiayi Tian, Hao Huang, Wen Guo, and Zhan Chen^{*©}

Department of Chemistry, University of Michigan, Ann Arbor, Michigan 48109, United States

Supporting Information



ABSTRACT: Graphene-based biosensors have attracted considerable attention due to their advantages of label-free detection and high sensitivity. Many such biosensors utilize noncovalent van der Waals force to attach proteins onto graphene surface while preserving graphene's high conductivity. Maintaining the protein structure without denaturation/substantial conformational change and controlling proper protein orientation on the graphene surface are critical for biosensing applications of these biosensors fabricated with proteins on graphene. Based on the knowledge we obtained from our previous experimental study and computer modeling of amino acid residual level interactions between graphene and peptides, here we systemically redesigned an important protein for better conformational stability and desirable orientation on graphene. In this paper, immunoglobulin G (IgG) antibody-binding domain of protein G (protein GB1) was studied to demonstrate how we can preserve the protein native structure and control the protein orientation on graphene surface by redesigning protein mutants. Various experimental tools including sum frequency generation vibrational spectroscopy, attenuated total refection-Fourier transform infrared spectroscopy, fluorescence spectroscopy, and circular dichroism spectroscopy were used to study the protein GB1 structure on graphene, supplemented by molecular dynamics simulations. By carefully designing the protein GB1 mutant, we can avoid strong unfavorable interactions between protein and graphene to preserve protein conformation and to enable the protein to adopt a preferred orientation. The methodology developed in this study is general and can be applied to study different proteins on graphene and beyond. With the knowledge obtained from this research, one could apply this method to optimize protein function on surfaces (e.g., to enhance biosensor sensitivity).

1. INTRODUCTION

Graphene is a two-dimensional (2D) material which has many excellent properties¹⁻³ and has been extensively applied in many applications such as graphene-based biosensors 4-6 and enzymatic biofuel cells, functional graphene nanomaterials for biointeractions,⁸ and protein separations.⁹ In such applications, biological molecules such as proteins directly interact with graphene, therefore it is extremely important to understand such relevant molecular interactions, for example, by characterizing the molecular structures of biological molecules on graphene. Particularly, it has been reported that biosensors using graphene as a platform, especially label-free biosensors based on graphene field-effect transistors (FET), have higher sensitivity, are easier to operate, and have simpler sample preparation processes compared to labeled biological sensors by fluorophores. 10-14 Understanding of graphene-biomolecule interaction will help to develop such biosensors with better performance.

Interfaces between graphene and biological molecules such as peptides and proteins have been of particular interest because of the chemical diversity that can be engineered into the interface, presenting the diversity of biological structure and function. 15 When modifying graphene surface with biomolecules, the interaction between graphene and biomolecules plays an important role in stabilizing the biomolecule conformation and determining biomolecule orientation on the graphene surface. Different from many other sensing materials where charge/hydrophobic interactions between protein amino acid residues and the material surfaces dominate, our previous work showed that interactions between peptides and a graphene surface depend mainly on the interactions of "planar" and hydrophilic residues in the peptide with graphene. The strong π - π interactions between the graphene surface and side chains of specific "planar" (e.g.,

Received: October 4, 2019 Published: November 27, 2019



aromatic) amino acids were reported by many experimental works and were parametrized in our study. 16 Therefore, different from various chemical binding methods applied for other popular biosensor materials such as self-assembled monolayers (SAMs), polymers, etc., immobilization of protein on graphene could be achieved by site specific mutations to manipulate the π - π interactions, which will be presented in detail below.

We demonstrated in our previous research 16 that an α helical peptide MSI-78 lies down on graphene. However, by carefully mutating two amino acids in MSI-78, we can minimize the π - π interaction between peptide aromatic amino acids and graphene to enable the mutant MSI-78 to tilt on the graphene surface. Such a mutation was designed by applying molecular dynamics (MD) simulations to calculate the peptide orientation on graphene with selected mutations. The simulated peptide orientation was validated using sum frequency generation (SFG) vibrational spectroscopy. Here, we would like to study the molecular behavior of a protein on graphene.

In this study, a well-studied protein GB1 was used as a model to investigate protein-graphene interaction by SFG and MD simulations. Protein GB1 is a domain of a cell surface protein called streptococcal protein G, which specifically binds to immunoglobulin G (IgG). Protein G has many applications and has been widely used in IgG purification or detection biosensors. 17-19 The binding mechanisms of the protein GB1 and IgG and the related controlling factors have been extensively investigated. Protein GB1 has also been widely used as a protein model to study protein folding/ unfolding with many experimental and simulation methods,^{23–27} including a recent simulation of GB1 on nanoparticles by Wei et al.²⁷ A fast and accurate simulation model was developed based on the thorough experimental measurements for protein GB1 and their interactions with solid material surfaces.2

Both our simulation results and experimental data show that graphene has strong interactions with the α -helical component of wild-type protein GB1 and eventually disrupts the α -helical structure in protein GB1 and denatures the protein. Such a phenomenon can be well explained by a high density of "planar" residues on the α -helix composition of GB1. As will be shown in detail below, the 56-residue protein GB1 contains 10 "planar" side-chain residues in total; such planar residues can strongly bind to the graphene surface.

By mutating two "planar" amino acids in the helical domain which have the smallest numbers of native contacts to alanine, we can retain the protein GB1 conformation by preserving the α -helical structure from destruction when in contact with graphene and maintaining the strong intramolecular connection between the α -helix and the β -strands and can control the protein GB1 orientation on the graphene surface. Combined experimental studies using CD, attenuated total reflection-Fourier transform infrared (ATR-FTIR), and SFG, and computational investigation with MD simulations using the coarse-grain model were performed to probe molecular interactions between protein GB1 and graphene. With the knowledge obtained from this research, we propose a generally applicable method to place proteins onto graphene without the need for chemical coupling to ensure that the proteins adopt native conformation and preferred orientation. This will be extremely important for designing and developing biosensors with graphene and biological molecules.

2. MATERIALS AND METHODS

- 2.1. Materials. Wild-type protein GB1 (sequence: MQY-KLILNGK TLKGETTTEA VDAATAEKVF KQYANDNGVD GEW-TYDDATK TFTVTE) and mutated protein GB1 (sequence: MOYKLILNGK TLKGETTTEA VDAATAEKVF KAYAADNGVD GEWTYDDATK TFTVTE) were ordered from Giotto Biotech (Sesto Fiorentino, Italy). Pristine monolayer graphene flakes were dispersed in ethanol solution. Graphene solution (1.0 mg/L) was purchased from Graphene Laboratories Inc. (Ronkonkoma, NY). The graphene surface preparation and characterization were described in our previous publication. 16 Right-angle CaF₂ prisms used for SFG experiments were purchased from Altos Photonics (Bozeman, MT).
- 2.2. Sum Frequency Generation Vibrational Spectroscopy. SFG theory and experimental details have been extensively reported²⁸⁻⁴³ and will not be repeated here. In this study, SFG experiments were performed using a commercial SFG system from EKSPLA. Briefly, the SFG system delivers picosecond (ps) pulsed lasers (20 ps pulse width) at a repetition rate of 50 Hz. One visible pulsed laser beam has a fixed wavelength at 532 nm, and the other infrared pulsed laser has a tunable wavelength (from 2.3 to 10 μ m). The visible and infrared pulses overlap spatially and temporally at the sample surface, then the SFG signal can be collected. A near total reflection geometry was used for data collection, as discussed previously. 44-47 Protein GB1 solution (0.1 mg/mL in 50 mM sodium phosphate solution, pH 5.5) was placed in contact with the graphenecoated CaF2 prism from the bottom. SFG spectra were collected with different polarization combinations of the input visible, input IR, and generated SFG beams, including ssp (s-polarized SFG signal, spolarized visible input, and p-polarized input IR) and ppp. More details about how to deduce protein orientation from SFG ssp and ppp spectra were extensively published previously, 33,48 discussions are presented in the Supporting Information.
- 2.3. Circular Dichroism Spectra Collection. The secondary structures of protein GB1 were measured by a J-1500 circular dichroism (CD) spectrometer (Jasco Inc., Japan) using a continuous scanning mode at room temperature. To use different graphene concentrations in the protein GB1 solution (0.01 mg/mL), different volumes of graphene solutions (5 mg/L) were added to a sample cell containing ~2 mL protein GB1 solution. The CD spectrum was collected between 240 and 190 nm at a 1 nm resolution and 50 nm/ min scan rate and averaged by five scans.
- 2.4. Attenuated Total Reflection Fourier Transform Infrared Spectroscopy. ATR-FTIR experiments were performed on a commercial Nicolet 6700 FTIR spectrometer. Graphene surface was deposited on Germanium ATR trapezoid prism (Crystran Ltd., Dorset, United Kingdom) coated with a thin layer of SiO₂. To avoid spectral confusion between the water O-H bending mode and protein GB1 amide-I mode, D2O instead of H2O was used in the ATR-FTIR measurements. Both s- and p-polarized ATR-FTIR spectra in the amide I frequency region were collected to determine the protein GB1 orientation. The background ATR-FTIR spectra were collected from graphene surface without protein GB1. Then, after protein GB1 was adsorbed onto the graphene surface, ATR-FTIR spectra were collected under the same condition using the previous spectra as backgrounds. More details about protein orientation determination from polarized ATR-FTIR spectra are presented in the previous publications.
- 2.5. Fluorescence Spectroscopy. A Jasco FP-6500 spectrofluorometer was used to measure tryptophan fluorescence spectra in protein GB1 solution (0.01 mg/mL). Different volumes of graphene solutions (10 mg/L) were added to a sample cell containing ~2 mL protein GB1 solution (0.01 mg/mL). Tryptophan emission spectra were collected from 300 to 400 nm with a 2.5 nm bandwidth and excitation at 285 nm.
- **2.6. Molecular Dynamics Simulations.** The coarse-grained MD simulation model to study interactions between protein molecules and surfaces with different hydrophobicities was originally developed by Wei and Knotts.⁵⁵ This model has been successfully applied to study interactions between various biological molecules and a variety of

Journal of the American Chemical Society

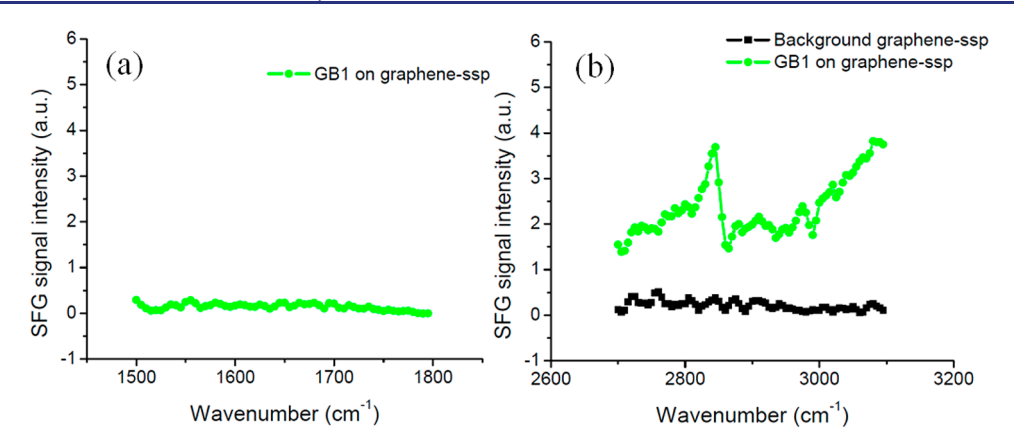


Figure 1. SFG spectra collected from the graphene/wild-type protein GB1 solution interface (a) in amide I frequency range and (b) in C-H stretching frequency range.

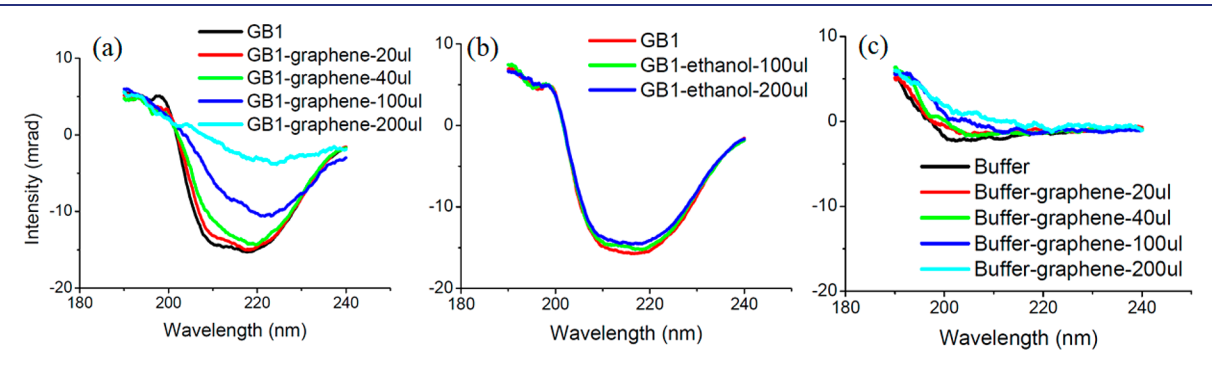


Figure 2. (a) CD spectra of GB1 solution (0.01 mg/mL) with different amounts of graphene solution (5 mg/L) in ethanol added. (b) Control CD spectra of GB1 solutions with different amounts of ethanol solutions (without graphene) added. (c) Control CD spectra of buffer solutions (without protein GB1) with different amounts of graphene solutions added.

surfaces where hydrophobic interactions play the major role. 27,51,54,56 This model was also optimized/parametrized to accommodate real experimental temperatures, accurately account for nanomaterial surface curvature, and $\pi - \pi$ interactions between amino acids with "planar" side chains and the graphene surface. 16,27

For this study, we focus on the graphene surface-protein interactions. Therefore, the particular version of the above model that emphasizes the $\pi - \pi$ interactions is used. ¹⁶ Specifically, the protein is described by the Karanicolas-Brooks (KB) Go-like model. A corresponding surface potential to each residue in the protein is formulated as

$$V_{graphene} = \sum_{i}^{N} \left\{ \pi \rho \sigma_{i}^{3} \varepsilon_{i} \left[\theta_{l} \left(\frac{\sigma_{i}}{z_{is}} \right)^{9} - \theta_{2} \left(\frac{\sigma_{i}}{z_{is}} \right)^{7} + \theta_{3} \left(\frac{\sigma_{i}}{z_{is}} \right)^{3} - (\theta_{x} + \theta_{p}(x_{pi} + 2 \times \delta)) \left(\frac{\sigma_{i}}{z_{is}} \right)^{3} \right] \right\}$$

$$(1)$$

where N is the residue number in the protein, $Z_{\rm is}$ is the distance between residue i and the surface, σ_i and ε_i are residue specific van der Waals parameters. The parameters (θ 's, Table S2) used in this work were determined by the previous studies. 16,27,55

The first three $\left(\frac{\sigma_i}{z_{is}}\right)^{x}$ terms in the above equation are the general terms to model amino acids of any type interacting with a solid surface, while the following terms in the equation are describing the differences of residues in terms of hydrophobicity and side chain planarity. As developed in a previous study, 27 we are able to scale the native contacts in protein GB1 so that we can perform the simulations at the experimental temperature of 298 K in this case with the NVT ensemble. Each simulation was performed with a time step of 1 fs and lasted for 100 ns. The protein initial pose above the surface was

randomly chosen, and the α -helix region was facing up, away from the graphene surface. Other simulation details can be found in the Support Information.

3. RESULTS AND DISCUSSION

3.1. Understanding Interactions between Wild-Type Protein GB1 and Graphene by Experiments. We have extensively investigated biological molecules chemically immobilized on surfaces and associated with model cell membranes using combined SFG and ATR-FTIR studies. 45-47,49-54 We also studied peptide orientation on graphene using SFG, supplemented by MD simulations. 16 In this study, we applied SFG and ATR-FTIR to examine molecular structures of protein GB1 on graphene, along with CD studies and MD simulations.

We have demonstrated that SFG technique is very powerful in determining orientations of biomolecules on surfaces. It can provide qualitative orientation information, that is, whether an α -helical peptide lies down on a surface or not. ¹⁶ It can also be used to quantitatively determine orientations of interfacial peptides and proteins versus the surface normal.⁴⁵ Here SFG signals were collected from the graphene/protein GB1 solution interface. Figure 1a shows the SFG amide I spectrum collected from the graphene/wild-type protein GB1 solution interface. We can see that the spectrum is featurelessly flat, or no SFG signal can be detected, showing either no protein GB1 is adsorbed to the graphene surface or the amide I groups in the adsorbed protein are disordered (or randomly oriented). Figure 1b shows the SFG spectrum collected from the same interface in the C-H stretching frequency range. Journal of the American Chemical Society

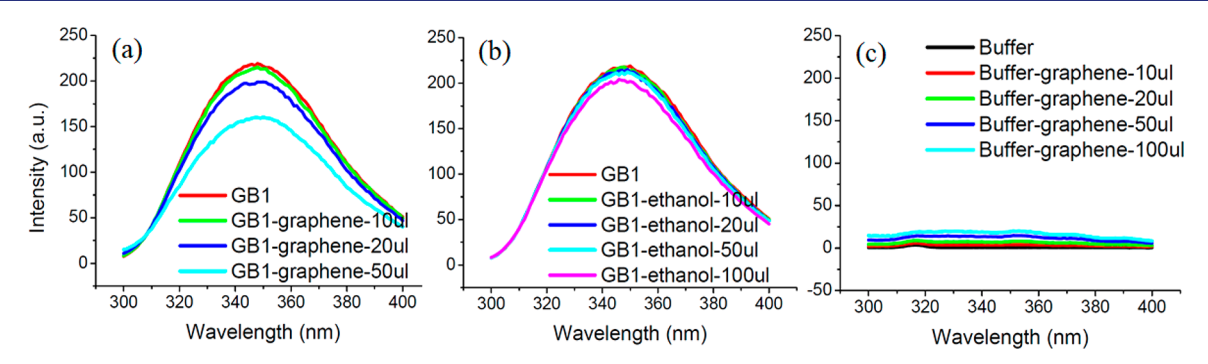


Figure 3. (a) Fluorescence spectra of GB1 solution (0.01 mg/mL) without and with different amounts of graphene solutions (10 mg/L) added. (b) Control fluorescence spectra of GB1 solution without and with different amounts of ethanol solutions (without graphene) added. (c) Control fluorescence spectra of buffer solutions (without protein GB1) without and with different amounts of graphene solutions added.

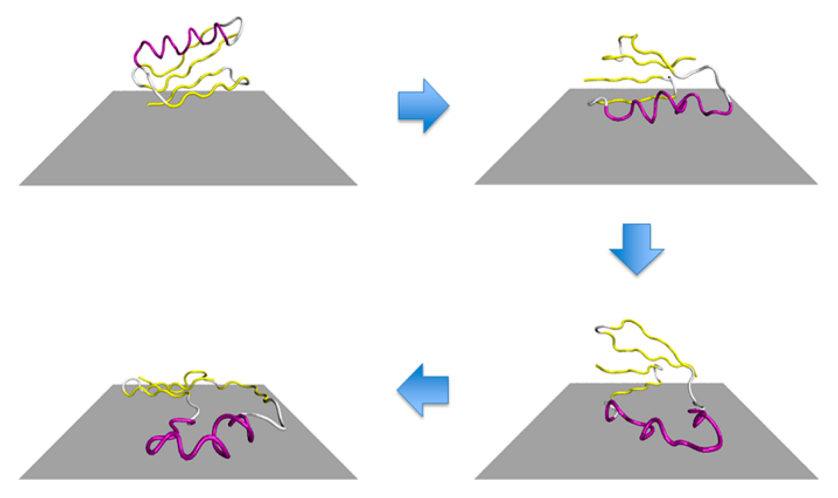


Figure 4. MD simulation results of wild-type protein GB1 adsorbed onto graphene surface.

Figure 1b shows that SFG signals from the C-H stretching modes can be clearly observed in the spectrum (the broad peak after 3000 cm⁻¹ is originated from the interface water molecules: the O-H stretching modes). These C-H stretching signals are contributed from protein side chain CH groups. This information indicates that protein GB1 can be adsorbed onto the graphene surface. The absence of the protein amide I signal is because of the disordered amide I groups in the protein, not the absence of the protein on graphene. The disordered amide I groups may come from randomly orientated protein GB1 on graphene or adsorbed protein GB1 on graphene with denatured structure (conformational change leading to disordered amide I groups). Since graphene is a well-defined 2D material, its surface is very ordered. Protein GB1 on graphene is unlikely randomly oriented with original folded conformation. Also if the adsorbed proteins are randomly orientated, SFG C-H stretching signal should be minimal as well, which was not what we observed. Therefore, the native protein GB1 must have adopted conformational changes on graphene.

To confirm that protein GB1 changes conformation after adsorbed to graphene, we performed CD spectroscopic studies. CD spectra were collected from protein GB1 aqueous solutions with different amounts of graphene solutions (in ethanol) added, as shown in Figure 2a. With more graphene added, more protein GB1 molecules were adsorbed to graphene. Figure 2a clearly shows that CD spectra changed greatly with the increased graphene amount added, indicating that protein GB1 adsorbed on graphene changed conforma-

tion. If the adsorbed protein GB1 and the GB1 in solution have the same conformation, CD spectra should not change when more graphene was added to the solution, which was not observed. To exclude the possibility that the CD spectral changes may be due to the added ethanol or graphene itself, we also collected CD spectra from protein GB1 solutions with different amounts of ethanol (without graphene added) (Figure 2b) and buffer solutions (without protein GB1) with different amounts of graphene added (Figure 2c). For both cases, CD spectral changes are minor. Therefore, the substantial CD spectral changes shown in Figure 2a are not caused by graphene or ethanol, but adsorbed protein GB1 on graphene instead. For the protein GB1 in solution, both α helical and β -sheet structures were detected by CD, the spectrum of which is shown in black in Figure 2a. The symbolic α -helix negative peak at \sim 208 nm gradually decreased as more graphene was added to the solution, indicating that the conformation change of protein GB1 after adsorbed to graphene involved loss of α -helical structure.

Strong interactions between protein GB1 and graphene have also been observed using fluorescence measurements. Figure 3a shows the fluorescence spectra of protein GB1 solution (0.01 mg/mL) with different amounts of graphene solutions added. We can clearly see that the intensity of the fluorescence signal decreased significantly when more graphene was added, which indicates that more and more protein GB1 molecules were adsorbed onto the graphene surface, resulting in graphene concentration-dependent fluorescence quenching. S7 As shown in a previous investigation, S7 protein GB1 adsorbed on latex

nanoparticles also demonstrated such a quenching effect. Since there is only one amino acid residue W43 contributing to the fluorescent signal, such a graphene quenching effect suggests that the environment around this residue changed upon adsorption to graphene. This residue is on the α -helical region of protein GB1, indicating the adsorption of the α -helical structure in protein GB1 to graphene, leading to the structural change of the α -helix, as evidenced by the CD studies presented above. Control fluorescence experiments on protein GB1 solutions with different amounts of ethanol solutions (without graphene) added (Figure 3b) and on buffer solutions (without protein GB1) with different amounts of graphene solutions added (Figure 3c) were also conducted. In both cases, fluorescence signal did not exhibit substantial changes, showing that the variation of ethanol or graphene in the solution does not markedly vary the fluorescence signal. This further supports that the above fluorescence signal change is due to the protein GB1 adsorption to graphene; more specifically, the α -helical domain adsorbed to graphene.

The combined experimental studies on wild-type protein GB1 and graphene interactions clearly indicated that protein GB1 molecules were adsorbed to the graphene surface with substantial conformational change.

3.2. Understanding Interactions between Wild-Type Protein GB1 and Graphene by Coarse-Grained MD **Simulations.** To understand more details of the interactions between protein GB1 and graphene, we performed MD simulations. The simulation results support the conclusion obtained from our above experimental measurements.

As shown in Figure 4, we initiated the MD simulation by placing the protein GB1 above the graphene surface with a distance of 1.6 nm. The initial pose of the protein was randomly chosen, and the α -helical region of the protein was far away from the graphene surface. As the simulation began, the protein was quickly adsorbed onto the graphene surface. The α -helix and one strand of the β -sheet in the protein contacted the graphene surface, while the other three β -sheets in the protein were above the graphene surface (no contact). At this point, the protein GB1 molecule still maintained most of its secondary and tertiary structures. As the simulation went on, the α -helix started to unwind on the graphene surface, and such a structural change led to the collapse of the whole protein structure. Eventually the entire protein was denatured and adsorbed onto the graphene surface.

Similar simulation methods were also applied to investigate interactions between the protein GB1 with latex nanospheres.²⁷ Different from that system, here the combination of the π - π interactions between the "planar" amino acid side chains and the graphene surface and the hydrophobic interactions govern the protein GB1-graphene interactions. As shown in Figure 5, the amino acid residues with "planar" side chains are highlighted in green for protein GB1. As we demonstrated in our previous work on peptide-graphene interactions, such "planar" amino acid residues have very high binding affinities with the graphene surface due to the favorable π – π interactions. Again, in the current study, this effect of strong $\pi - \pi$ interaction was parametrized into the coarse-grained KB Go-like model (which was well tested by the peptide-graphene interactions). As shown in Figure 5, five out of the 10 strong binding amino acids (to graphene) reside in the α -helix, while the other five are spread around the protein in the coil or β -sheet regions. Due to the specific strong binding affinity with the graphene surface, the high density of

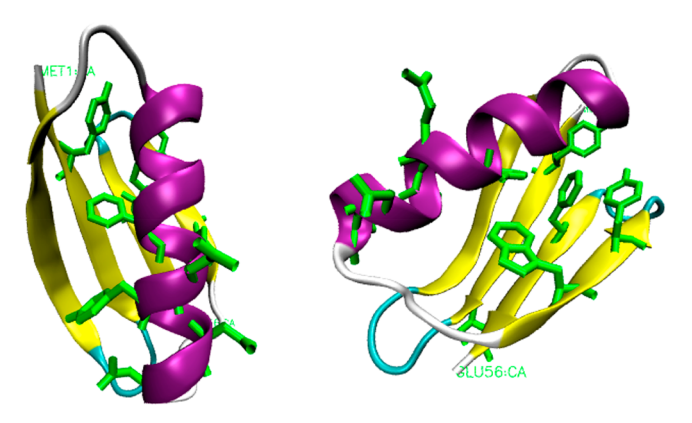


Figure 5. Protein GB1 structure (α-helix in purple and β-sheets in yellow) with highlighted "planar" side chain residues in green sticks.

the "planar" side-chain residues in the α -helix results in the adsorption of the α -helical domain to the graphene surface. The strong interactions between these amino acids in helix and graphene lead to denaturation of the protein GB1 on graphene, as observed in MD simulations as well as the experimental measurements.

3.3. Redesign of the Protein GB1 for Better Stability on Graphene. Based on the experimental measurements and MD simulations presented above, we know that the wild-type protein GB1 underwent substantial conformational changes on graphene, due to strong protein GB1-graphene interactions. Here by changing the protein-graphene interactions through protein engineering, we hope to improve the protein stability on graphene. As presented above, the high density of "planar" side chain residues leads to the strong interactions between the α -helical region in protein GB1 and the graphene surface, which accounts for the protein denaturation. Therefore, an obvious protein mutation strategy is to reduce the number of the "planar" side chain residues in the α -helix to decrease the protein-graphene interaction. We can certainly mutate all the five "planar" amino acids in the helix. After the following analysis, we found that it is not necessary to do so. As shown in Figure 5, three out of the five "planar" side-chain residues in the α -helix are interfacing with other residues on the β -sheets in the protein. The other two "planar" amino acids have their side-chains extending out and interfacing with the solvent, which likely will have strong interactions with graphene (at least initially) when the protein interacts with the graphene surface. Thus, choosing these two residues for mutation should be a good strategy to weaken protein GB1-graphene interactions.

The minimum mutation number of the amino acids should have the least impact on the original protein structure. Therefore, before performing research on protein GB1 with the above two amino acids mutated, single-point mutations (Q32A or N35A) on protein GB1 for the above two "planar" amino acid candidate residues were performed. For simulations, the protein mutations were performed with MMTSB tools⁵⁸ (http://www.mmtsb.org), and the resulting structure energies were minimized using Charmm. Following the energy minimization, coarse-grained MD simulations were performed on mutant GB1 with single mutations adsorbed onto graphene surface, with the same simulation conditions as those used for the wild-type GB1 presented above. However, the simulation results indicated that the single mutation for either candidate residue is not sufficient in changing the protein behavior on the



Figure 6. Initial and final snapshots of the double-point mutated protein GB1 on graphene from an example simulation.

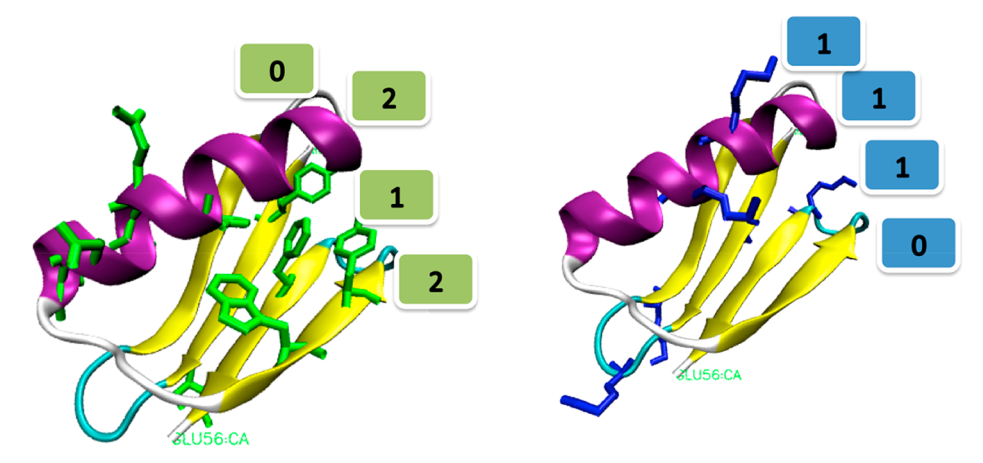


Figure 7. Distribution of "planar" side-chain residues (left) and lysines (right) in β -sheet regions of protein GB1 that determines the adsorbed orientation of the protein GB1 mutant.

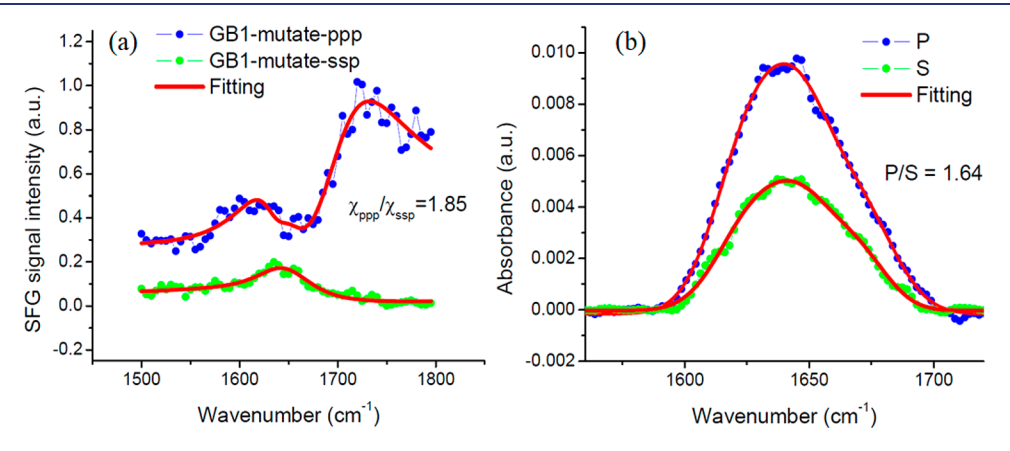


Figure 8. (a) SFG and (b) polarized ATR-FTIR spectra of mutated GB1 on graphene.

graphene surface. Same protein pose and denatured structures were obtained from the simulations. We therefore decided to further reduce the number of the "planar" side chain residues in the α -helix to weaken the protein—graphene interaction and performed the double-point mutations Q32A and N35A for protein GB1.

After performing the two-point mutation in the sequence of the wild-type protein GB1, we carried out MD simulations to study such a mutated protein GB1 on graphene. As shown in Figure 6, the protein GB1 was adsorbed onto the graphene surface with a side-on pose and a well-maintained structure. The α -helix was much less disturbed with one end adsorbed on the surface, while the other end was far away from the surface with the support of the β -sheets in the protein. Such a pose can be stable also because the "planar" side-chain residues and the hydrophilic residues are distributed in different domains. As shown in Figure 7, the β -sheet adsorbed onto the graphene surface has two "planar" side-chain residues (Trp 43 and Tyr 45) but no Lys (K) residues. As we demonstrated in our

previous studies on peptide— MoS_2 interactions, Lys residues preferred to be exposed to water (instead of interacting with the surface). On the contrary, the β -sheet far away from the graphene surface has none "planar" side-chain residue but one Lys (K) residue. This result is consistent with our previous studies on the interactions between graphene and the α -helical peptide MSI-78. 16

Our MD simulation results predicted a conserved conformation and preferred orientation for protein GB1 mutant (with only two amino acids mutated) on graphene. To confirm the simulation conclusion, we performed experimental measurements on such a protein GB1 mutant on graphene. With such a well-maintained conformation and well-ordered orientation with the α -helical structure more or less standing up (or tilting) on graphene, we should be able to detect amide I signals from the protein GB1 mutant on graphene using SFG. Both SFG and ATR-FTIR were applied to study interactions between mutant protein GB1 and graphene.

Journal of the American Chemical Society

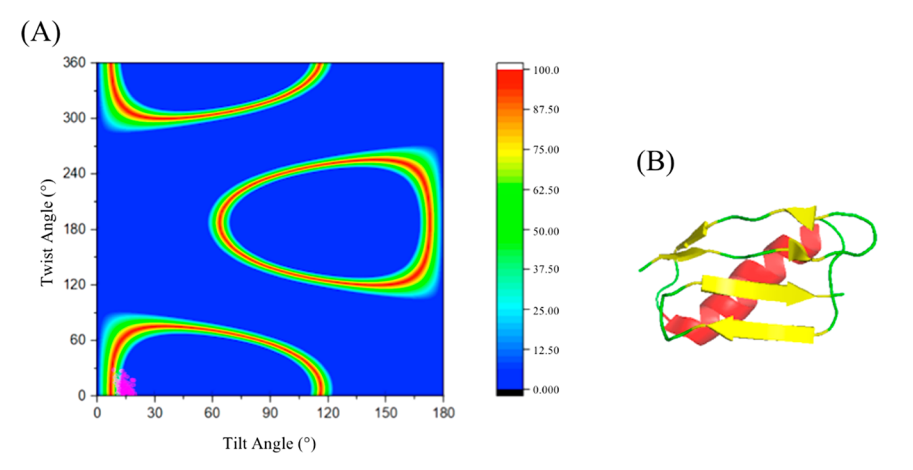


Figure 9. (A) Heat map plot of possible orientation angle regions deduced using the SFG and ATR-FTIR measurements. Pink dots are the obtained orientations from the final 5 ns of MD simulation. (B) The averaged orientation ($\theta = 14^{\circ}$, $\psi = 8^{\circ}$) of protein GB1 on graphene surface from the final 5 ns of simulation.

Figure 8a shows the SFG spectra of the mutated GB1 protein on graphene collected using the ssp and ppp polarization combinations. The spectra were fitted, and the fitted amide I peak for each spectrum is centered at ~1650 cm⁻¹, which is originated from the α -helical structure in the mutant protein GB1. The fitted SFG signal strength ratio indicates that $\chi^{(2)}_{ppp}/\chi^{(2)}_{ssp}=1.85$, which can be used to determine the protein GB1 mutant orientation on the graphene surface. The details of protein orientation determination have been described in previous publications and will not be repeated here. 48,50-53 Polarized ATR-FTIR spectra were also collected from the mutant protein GB1 on graphene, which are presented in Figure 8b. Gaussian functions were used to fit these spectra and decompose the spectra into the components contributed by α -helices, β -sheets, and random coil structures. We calculated the polarized ratio of α -helices and used it to determine the protein orientation. The method used to study protein orientation with ATR-FTIR spectra was also extensively published. 50-54

With SFG and ATR-FTIR spectral fitting results, we can deduce the protein orientation (specified by a combination of the tilt (θ) and the twist angles (ψ) on graphene surface. The zero orientation position ($\theta = 0^{\circ}$, $\psi = 0^{\circ}$) was defined as the orientation of the protein in the PDB file 1GB1. Figure 9a shows the heat map of the possible orientations matching between predicted SFG/ATR-FTIR data and SFG/ATR-FTIR experimentally measured data, with the color indicating the matching probability. The calculation of the heat map includes a 20% error bar; that is, in the heat map, 100% for the orientation matching means the calculated and the measured values exactly match, shown in red. If the calculated and measured data have 20% difference or more, the matching score is 0%, shown in blue. If the difference is 10%, then the matching score is (20% - 10%)/20% = 50%, shown in green. The detailed description of the heat map generation was published^{48,53} and will not be repeated again. To correlate the experimentally measured orientation to that obtained from the MD simulations, we also plot the protein orientations obtained from the final 5 ns simulation as small pink dots on the heat map. The simulated data can match the experimentally deduced orientation angle region which has small tilt and twist angles (see Supporting Information). Figure 9b shows the averaged orientation ($\theta = 14^{\circ}$, $\psi = 8^{\circ}$) of simulated

orientations in the final 5 ns, with α -helix standing up (or tilting) on the graphene surface. It is worth mentioning that for the protein GB1 orientation analysis, we assumed that the conformation of the protein GB1 mutant is the same as the protein GB1 crystal structure. This assumption is more or less reasonable, which can be validated using the MD simulation results shown in Figure 6: The protein–surface interaction induced very slight structural distortion.

4. CONCLUSIONS

Graphene-based biosensors have been extensively researched and have many potential applications in biodetection with high sensitivity and selectivity. Retaining the biomolecule's native conformation and controlling biomolecule's orientation on graphene are two important aspects for improving the performance of biosensors constructed with graphene and proteins, but are very challenging tasks. In this study, we chose protein GB1, an immunoglobulin G (IgG) antibody-binding domain of protein G, as a model protein to demonstrate that we can preserve the protein native structure and control protein orientation after adsorbed onto the graphene surface. The combined experimental and simulation approach adopted in this research allows us to probe the detailed molecular interactions between protein molecules and graphene. We found that such interactions could destroy the α -helix structure of the wild-type protein GB1 on graphene, leading to the denaturation of the entire protein. After carefully analyzing the protein-graphene interactions, we designed a protein GB1 mutant with only two amino acids in the α -helical structure mutated. Our MD simulations indicated that we could preserve the protein conformation and control its orientation on the graphene surface by such small changes made in the protein sequence. It is necessary to mention that it is important to ensure that the mutations on protein will not negatively change the protein function. In the past, we showed that it is feasible to maintain the protein activity by selective mutations to improve the surface immobilization.⁶⁰

The approach developed in this study is widely applicable to investigate interactions between graphene and other protein molecules and design proteins which can adopt native conformation and preferred orientation on graphene. This method can also be used to study detailed molecular

interactions between proteins and surfaces of other materials such as other 2D materials, SAMs, polymers, etc.

ASSOCIATED CONTENT

S Supporting Information

The Supporting Information is available free of charge at https://pubs.acs.org/doi/10.1021/jacs.9b10705.

SFG and ATR-FTIR spectra peak fitting parameters, MD simulation method, possible protein orientations, and heat map with related tilt and twist angles (PDF)

AUTHOR INFORMATION

Corresponding Author

*zhanc@umich.edu

ORCID

Xingquan Zou: 0000-0002-9716-9771 Zhan Chen: 0000-0001-8687-8348

Author Contributions

[†]These authors contributed equally to this paper.

Notes

The authors declare no competing financial interest.

ACKNOWLEDGMENTS

This research was supported by the National Science Foundation (CHE-1505385, CHE-1904380). We thank NVIDIA Corporation for the donation of the Quadro P6000 GPU which was used for this research.

■ REFERENCES

- (1) Allen, M. J.; Tung, V. C.; Kaner, R. B. Honeycomb Carbon: A Review of Graphene. *Chem. Rev.* **2010**, *110* (1), 132–145.
- (2) Lin, L.; Deng, B.; Sun, J.; Peng, H.; Liu, Z. Bridging the Gap between Reality and Ideal in Chemical Vapor Deposition Growth of Graphene. *Chem. Rev.* **2018**, *118* (18), 9281–9343.
- (3) Kozbial, A.; Zhou, F.; Li, Z.; Liu, H.; Li, L. Are Graphitic Surfaces Hydrophobic? *Acc. Chem. Res.* **2016**, 49 (12), 2765–2773.
- (4) Zheng, Q.; Wu, H.; Wang, N.; Yan, R.; Ma, Y.; Guang, W.; Wang, J.; Ding, K. Graphene-Based Biosensors for Biomolecules Detection. *Curr. Nanosci.* **2014**, *10* (5), *627*–*637*.
- (5) Patil, A. V.; Fernandes, F. B.; Bueno, P. R.; Davis, J. J. Graphene-Based Protein Biomarker Detection. *Bioanalysis* **2015**, 7 (6), 725–742.
- (6) Wang, L.; Xiong, Q.; Xiao, F.; Duan, H. 2D Nanomaterials Based Electrochemical Biosensors for Cancer Diagnosis. *Biosens. Bioelectron.* **2017**, *89*, 136–151.
- (7) Karimi, A.; Othman, A.; Uzunoglu, A.; Stanciu, L.; Andreescu, S. Graphene Based Enzymatic Bioelectrodes and Biofuel Cells. *Nanoscale* **2015**, *7* (16), 6909–6923.
- (8) Cheng, C.; Li, S.; Thomas, A.; Kotov, N. A.; Haag, R. Functional Graphene Nanomaterials Based Architectures: Biointeractions, Fabrications, and Emerging Biological Applications. *Chem. Rev.* **2017**, *117* (3), 1826–1914.
- (9) Chen, X.; Hai, X.; Wang, J. Graphene/Graphene Oxide and Their Derivatives in the Separation/Isolation and Preconcentration of Protein Species: A Review. *Anal. Chim. Acta* **2016**, *922*, 1–10.
- (10) Ohno, Y.; Maehashi, K.; Matsumoto, K. Label-Free Biosensors Based on Aptamer-Modified Graphene Field-Effect Transistors. *J. Am. Chem. Soc.* **2010**, *132* (51), 18012–18013.
- (11) Singh, M.; Holzinger, M.; Tabrizian, M.; Winters, S.; Berner, N. C.; Cosnier, S.; Duesberg, G. S. Noncovalently Functionalized Monolayer Graphene for Sensitivity Enhancement of Surface Plasmon Resonance Immunosensors. *J. Am. Chem. Soc.* **2015**, *137* (8), 2800–2803.

- (12) Chou, S. S.; De, M.; Luo, J.; Rotello, V. M.; Huang, J.; Dravid, V. P. Nanoscale Graphene Oxide (NGO) as Artificial Receptors: Implications for Biomolecular Interactions and Sensing. *J. Am. Chem. Soc.* **2012**, *134* (40), 16725–16733.
- (13) Matsumoto, K.; Maehashi, K.; Ohno, Y.; Inoue, K. Recent Advances in Functional Graphene Biosensors. *J. Phys. D: Appl. Phys.* **2014**, *47* (9), 094005.
- (14) Ohno, Y.; Maehashi, K.; Yamashiro, Y.; Matsumoto, K. Electrolyte-Gated Graphene Field-Effect Transistors for Detecting PH and Protein Adsorption. *Nano Lett.* **2009**, *9* (9), 3318–3322.
- (15) Russell, S. R.; Claridge, S. A. Peptide Interfaces with Graphene: An Emerging Intersection of Analytical Chemistry, Theory, and Materials. *Anal. Bioanal. Chem.* **2016**, 408 (11), 2649–2658.
- (16) Zou, X.; Wei, S.; Jasensky, J.; Xiao, M.; Wang, Q.; Brooks, C. L., III; Chen, Z. Molecular Interactions between Graphene and Biological Molecules. *J. Am. Chem. Soc.* **2017**, *139* (5), 1928–1936.
- (17) Chen, W.; Lei, Y.; Li, C. M. Regenerable Leptin Immunosensor Based on Protein G Immobilized Au-Pyrrole Propylic Acid-Polypyrrole Nanocomposite. *Electroanalysis* **2010**, 22 (10), 1078–1083.
- (18) Page, M.; Thorpe, R. Purification of IgG Using Protein A or Protein G. In *The Protein Protocols Handbook*; Walker, J. M., Ed.; Humana Press: Totowa, NJ, 2002; pp 993–994.
- (19) Bailey, L. J.; Sheehy, K. M.; Hoey, R. J.; Schaefer, Z. P.; Ura, M.; Kossiakoff, A. A. Applications for an Engineered Protein-G Variant with a PH Controllable Affinity to Antibody Fragments. *J. Immunol. Methods* **2014**, *415*, 24–30.
- (20) Sloan, D. J.; Hellinga, H. W. Dissection of the Protein G B1 Domain Binding Site for Human IgG Fc Fragment. *Protein Sci.* **1999**, 8 (8), 1643–1648.
- (21) Watanabe, H.; Matsumaru, H.; Ooishi, A.; Feng, Y.; Odahara, T.; Suto, K.; Honda, S. Optimizing PH Response of Affinity between Protein G and IgG Fc: How Electrostatic Modulations Affect Protein-Protein Interactions. *J. Biol. Chem.* **2009**, 284 (18), 12373–12383.
- (22) Öster, C.; Kosol, S.; Hartlmüller, C.; Lamley, J. M.; Iuga, D.; Oss, A.; Org, M.-L.; Vanatalu, K.; Samoson, A.; Madl, T.; Lewandowski, J. R. Characterization of Protein—Protein Interfaces in Large Complexes by Solid-State NMR Solvent Paramagnetic Relaxation Enhancements. J. Am. Chem. Soc. 2017, 139 (35), 12165—12174.
- (23) Morrone, A.; Giri, R.; Toofanny, R. D.; Travaglini-Allocatelli, C.; Brunori, M.; Daggett, V.; Gianni, S. GB1 Is Not a Two-State Folder: Identification and Characterization of an On-Pathway Intermediate. *Biophys. J.* **2011**, *101* (8), 2053–2060.
- (24) Harrison, E. T.; Weidner, T.; Castner, D. G.; Interlandi, G. Predicting the Orientation of Protein G B1 on Hydrophobic Surfaces Using Monte Carlo Simulations. *Biointerphases* **2017**, *12* (2), 02D401.
- (25) Berkovich, R.; Mondal, J.; Paster, I.; Berne, B. J. Simulated Force Quench Dynamics Shows GB1 Protein Is Not a Two State Folder. J. Phys. Chem. B 2017, 121 (20), 5162–5173.
- (26) Karanicolas, J.; Brooks, C. L., III The Origins of Asymmetry in the Folding Transition States of Protein L and Protein G. *Protein Sci.* **2002**, *11* (10), 2351–2361.
- (27) Wei, S.; Ahlstrom, L. S.; Brooks, C. L., III Exploring Protein-Nanoparticle Interactions with Coarse-Grained Protein Folding Models. *Small* **2017**, *13* (18), 1603748.
- (28) Lu, X.; Zhang, C.; Ulrich, N.; Xiao, M.; Ma, Y.-H.; Chen, Z. Studying Polymer Surfaces and Interfaces with Sum Frequency Generation Vibrational Spectroscopy. *Anal. Chem.* **2017**, 89 (1), 466–489.
- (29) Zhuang, X.; Miranda, P. B.; Kim, D.; Shen, Y. R. Mapping Molecular Orientation and Conformation at Interfaces by Surface Nonlinear Optics. *Phys. Rev. B: Condens. Matter Mater. Phys.* **1999**, 59 (19), 12632–12640.
- (30) Chen, Z.; Shen, Y. R.; Somorjai, G. A. Studies of Polymer Surfaces by Sum Frequency Generation Vibrational Spectroscopy. *Annu. Rev. Phys. Chem.* **2002**, *53* (1), 437–465.
- (31) Moad, A. J.; Simpson, G. J. A Unified Treatment of Selection Rules and Symmetry Relations for Sum-Frequency and Second

- Harmonic Spectroscopies. J. Phys. Chem. B 2004, 108 (11), 3548-3562.
- (32) Mikhnenko, O. V.; Cordella, F.; Sieval, A. B.; Hummelen, J. C.; Blom, P. W. M.; Loi, M. A. Temperature Dependence of Exciton Diffusion in Conjugated Polymers. *J. Phys. Chem. B* **2008**, *112* (37), 11601–11604.
- (33) Nguyen, K. T.; Le Clair, S. V.; Ye, S.; Chen, Z. Orientation Determination of Protein Helical Secondary Structures Using Linear and Nonlinear Vibrational Spectroscopy. *J. Phys. Chem. B* **2009**, *113* (36), 12169–12180.
- (34) Shen, Y. R. Surface Properties Probed by Second-Harmonic and Sum-Frequency Generation. *Nature* **1989**, 337 (6207), 519–525.
- (35) Jung, S.-Y.; Lim, S.-M.; Albertorio, F.; Kim, G.; Gurau, M. C.; Yang, R. D.; Holden, M. A.; Cremer, P. S. The Vroman Effect: A Molecular Level Description of Fibrinogen Displacement. *J. Am. Chem. Soc.* **2003**, 125 (42), 12782–12786.
- (36) Lutz, H.; Jaeger, V.; Schmüser, L.; Bonn, M.; Pfaendtner, J.; Weidner, T. The Structure of the Diatom Silaffin Peptide R5 within Freestanding Two-Dimensional Biosilica Sheets. *Angew. Chem., Int. Ed.* **2017**, *56* (28), 8277–8280.
- (37) Tan, J.; Zhang, J.; Li, C.; Luo, Y.; Ye, S. Ultrafast Energy Relaxation Dynamics of Amide I Vibrations Coupled with Protein-Bound Water Molecules. *Nat. Commun.* **2019**, *10* (1), 1010.
- (38) Weidner, T.; Apte, J. S.; Gamble, L. J.; Castner, D. G. Probing the Orientation and Conformation of α -Helix and β -Strand Model Peptides on Self-Assembled Monolayers Using Sum Frequency Generation and NEXAFS Spectroscopy. *Langmuir* **2010**, 26 (5), 3433–3440.
- (39) Yan, E. C. Y.; Fu, L.; Wang, Z.; Liu, W. Biological Macromolecules at Interfaces Probed by Chiral Vibrational Sum Frequency Generation Spectroscopy. *Chem. Rev.* **2014**, *114* (17), 8471–8498.
- (40) Li, Q.; Kuo, C. W.; Yang, Z.; Chen, P.; Chou, K. C. Surface-Enhanced IR-Visible Sum Frequency Generation Vibrational Spectroscopy. *Phys. Chem. Chem. Phys.* **2009**, *11* (18), 3436.
- (41) Premadasa, U. I.; Adhikari, N. M.; Baral, S.; Aboelenen, A. M.; Cimatu, K. L. A. Conformational Changes of Methacrylate-Based Monomers at the Air–Liquid Interface Due to Bulky Substituents. *J. Phys. Chem. C* **2017**, *121* (31), 16888–16902.
- (42) Ye, H.; Abu-Akeel, A.; Huang, J.; Katz, H. E.; Gracias, D. H. Probing Organic Field Effect Transistors In Situ during Operation Using SFG. J. Am. Chem. Soc. 2006, 128 (20), 6528–6529.
- (43) Perry, A.; Neipert, C.; Space, B.; Moore, P. B. Theoretical Modeling of Interface Specific Vibrational Spectroscopy: Methods and Applications to Aqueous Interfaces. *Chem. Rev.* **2006**, *106* (4), 1234–1258.
- (44) Wang, J.; Even, M. A.; Chen, X.; Schmaier, A. H.; Waite, J. H.; Chen, Z. Detection of Amide I Signals of Interfacial Proteins in Situ Using SFG. J. Am. Chem. Soc. 2003, 125 (33), 9914–9915.
- (45) Wang, Q.; Wei, S.; Wu, J.; Zou, X.; Sieggreen, O.; Liu, Y.; Xi, C.; Brooks, C. L., III; Chen, Z. Interfacial Behaviors of Antimicrobial Peptide Cecropin P1 Immobilized on Different Self-Assembled Monolayers. J. Phys. Chem. C 2015, 119 (39), 22542–22551.
- (46) Li, Y.; Zhang, X.; Myers, J.; Abbott, N. L.; Chen, Z. Room Temperature Freezing and Orientational Control of Surface-Immobilized Peptides in Air. *Chem. Commun.* **2015**, *51* (55), 11015–11018.
- (47) Wei, S.; Zou, X.; Cheng, K.; Jasensky, J.; Wang, Q.; Li, Y.; Hussal, C.; Lahann, J.; Brooks, C. L., III; Chen, Z. Orientation Determination of a Hybrid Peptide Immobilized on CVD-Based Reactive Polymer Surfaces. *J. Phys. Chem. C* **2016**, *120* (34), 19078–19086
- (48) Boughton, A. P.; Yang, P.; Tesmer, V. M.; Ding, B.; Tesmer, J. J. G.; Chen, Z. Heterotrimeric G Protein γ1γ2 Subunits Change Orientation upon Complex Formation with G Protein-Coupled Receptor Kinase 2 (GRK2) on a Model Membrane. *Proc. Natl. Acad. Sci. U. S. A.* **2011**, 108 (37), E667–673.
- (49) Jasensky, J.; Ferguson, K.; Baria, M.; Zou, X.; McGinnis, R.; Kaneshiro, A.; Badieyan, S.; Wei, S.; Marsh, E. N. G.; Chen, Z.

- Simultaneous Observation of the Orientation Structure and Activity of Surface-Immobilized Enzymes. *Langmuir* **2018**, 34 (31), 9133–9140.
- (50) Liu, Y.; Ogorzalek, T. L.; Yang, P.; Schroeder, M. M.; Marsh, E. N. G.; Chen, Z. Molecular Orientation of Enzymes Attached to Surfaces through Defined Chemical Linkages at the Solid–Liquid Interface. J. Am. Chem. Soc. 2013, 135 (34), 12660–12669.
- (51) Zou, X.; Wei, S.; Badieyan, S.; Schroeder, M.; Jasensky, J.; Brooks, C. L., III; Marsh, E. N. G.; Chen, Z. Investigating the Effect of Two-Point Surface Attachment on Enzyme Stability and Activity. *J. Am. Chem. Soc.* **2018**, *140* (48), 16560–16569.
- (52) Shen, L.; Schroeder, M.; Ogorzalek, T. L.; Yang, P.; Wu, F.-G.; Marsh, E. N. G.; Chen, Z. Surface Orientation Control of Site-Specifically Immobilized Nitro-Reductase (NfsB). *Langmuir* **2014**, *30* (20), 5930–5938.
- (53) Yang, P.; Boughton, A.; Homan, K.; Tesmer, J.; Chen, Z. Membrane Orientation of $G\alpha i\beta 1\gamma 2$ and $G\beta 1\gamma 2$ Determined via Combined Vibrational Spectroscopic Studies. *J. Am. Chem. Soc.* **2013**, 135 (13), 5044–5051.
- (54) Xiao, M.; Wei, S.; Chen, J.; Tian, J.; Brooks, C. L., III; Marsh, E. N. G.; Chen, Z. Molecular Mechanisms of Interactions between Monolayered Transition Metal Dichalcogenides and Biological Molecules. J. Am. Chem. Soc. 2019, 141 (25), 9980–9988.
- (55) Wei, S.; Knotts, T. A. A Coarse Grain Model for Protein-Surface Interactions. *J. Chem. Phys.* **2013**, *139* (9), 095102.
- (56) Wei, S.; Brooks, C. L., III Stability and Orientation of Cecropin P1 on Maleimide Self-Assembled Monolayer (SAM) Surfaces and Suggested Functional Mutations. *Chin. Chem. Lett.* **2015**, 26 (4), 485–490.
- (57) Pan, H.; Qin, M.; Meng, W.; Cao, Y.; Wang, W. How Do Proteins Unfold upon Adsorption on Nanoparticle Surfaces? *Langmuir* **2012**, 28 (35), 12779–12787.
- (58) Feig, M.; Karanicolas, J.; Brooks, C. L., III MMTSB Tool Set: Enhanced Sampling and Multiscale Modeling Methods for Applications in Structural Biology. *J. Mol. Graphics Modell.* **2004**, 22, 377–395.
- (59) Xiao, M.; Wei, S.; Li, Y.; Jasensky, J.; Chen, J.; Brooks, C. L., III; Chen, Z. Molecular Interactions between Single Layered MoS₂ and Biological Molecules. *Chem. Sci.* **2018**, *9* (7), 1769–1773.
- (60) Shen, L.; Schroeder, M.; Ogorzalek, T. L.; Yang, P.; Wu, F.; Marsh, E. N. G.; Chen, Z. Surface Orientation Control of Site-Specifically Immobilized Nitro-reductase (NsfB). *Langmuir* **2014**, *30* (20), 5930–5938.